

Generic Two-Phase Coexistence and Nonequilibrium Criticality in a Lattice Version of Schlögl's Second Model for Autocatalysis

Da-Jiang Liu

Received: 19 November 2008 / Accepted: 25 February 2009 / Published online: 14 March 2009
© Springer Science+Business Media, LLC 2009

Abstract A two-dimensional atomistic realization of Schlögl's second model for autocatalysis is implemented and studied on a square lattice as a prototypical nonequilibrium model with first-order transition. The model has no explicit symmetry and its phase transition can be viewed as the nonequilibrium counterpart of liquid-vapor phase separations. We show some familiar concepts from study of equilibrium systems need to be modified. Most importantly, phase coexistence can be a generic feature of the model, occurring over a finite region of the parameter space. The first-order transition becomes continuous as a temperature-like variable increases. The associated critical behavior is studied through Monte Carlo simulations and shown to be in the two-dimensional Ising universality class. However, some common expectations regarding finite-size corrections and fractal properties of geometric clusters for equilibrium systems seems to be inapplicable.

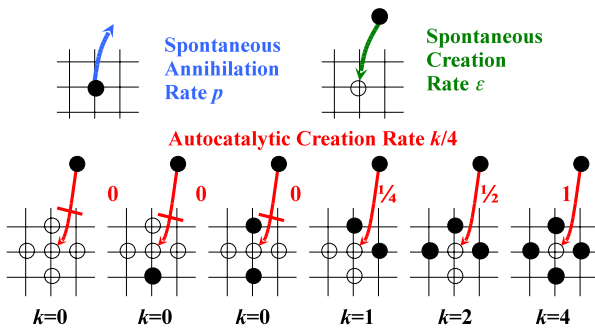
Keywords Nonequilibrium phase transition · Generic phase coexistence · Ising universality class · Percolation

1 Introduction

Lattice models with irreversible dynamics has been studied extensively in recent years to reveal fundamental properties of nonequilibrium phase transitions [1–3]. The behavior of steady-states in these models is often at least superficially quite similar to that of equilibrium systems with the same symmetry and spatial dimension. In particular, it has been shown that the critical transition in systems with two-phase coexistence and without absorbing states belongs to the Ising universality class. While most of the models studied possess direct “up-down” symmetry [4, 5], models without explicit symmetry that are used to model surface reactions has also been shown [6–8] to belong to the Ising universality class when adspecies diffusion is limited. Similarities to equilibrium systems also extends to metastabilities and transitions between the two phases below the critical point [9, 10].

D.-J. Liu (✉)
Ames Laboratory—USDOE, Iowa State University, Ames, IA 50011, USA
e-mail: dajiang@fi.ameslab.gov

Fig. 1 (Color online) Schematic of particle (denoted by black circles) spontaneous annihilation, spontaneous creation, and catalytic creation in a lattice-gas realization of Schlögl's second model



Recently, a simple lattice-gas model based on quadratic contact processes [11] has been shown [12–14] to have an interface-orientation-dependent discontinuous transition and generic two-phase coexistence that occurs over a range of parameters, in stark contrast to behavior in equilibrium systems. There, the focus is on the limit where one of the phase is an absorbing state. In this paper, we introduce a finite temperature-like variable and focus on the critical point of the system.

For this analysis, we will consider a stochastic realization of Schlögl's second model for autocatalysis describing the creation and annihilation of a population of particles X . The traditional *mean-field formulation* of the general form of Schlögl's second model [15] includes the steps: $\emptyset \leftrightarrow X$ (spontaneous creation and annihilation of particles) and $2X \leftrightarrow 3X$ (autocatalytic creation and annihilation of particles). Our *lattice-gas formulation*, where particles are located at sites of a square lattice, includes the following steps: $X \rightarrow \emptyset$ at rate p (spontaneous annihilation); $\emptyset \rightarrow X$ at a “small” rate ϵ (spontaneous creation); $\emptyset + 2X \rightarrow 3X$ at rate $k/4$, where k is the number of diagonal nearest-neighbor (NN) pairs of particle X which are adjacent to \emptyset (autocatalytic creation) [11–13]. See Fig. 1 for a schematic. The explicit “population-limiting reaction” $3X \rightarrow 2X$ in the traditional mean-field formulation is not needed in the lattice version as population increase is limited by availability of empty sites.

It is an easy matter then to write down the mean-field rate equation for the evolution of the particle density ρ ,

$$d\rho/dt = \epsilon(1 - \rho) - p\rho + (1 - \rho)\rho^2. \quad (1)$$

The stationary solution given by requiring $d\rho/dt = 0$ in (1) can be written as

$$p = [\epsilon(1 - \rho) + \rho^2 - \rho^3]/\rho. \quad (2)$$

It can be shown that for $\epsilon < \epsilon_c = 1/27$, there exists a range of p values that (1) has three stationary solutions, two of them stable, and one of them unstable. This is analogous to the solution of the van der Waals equation below the critical temperature where there is coexistence of liquid and vapor phases.

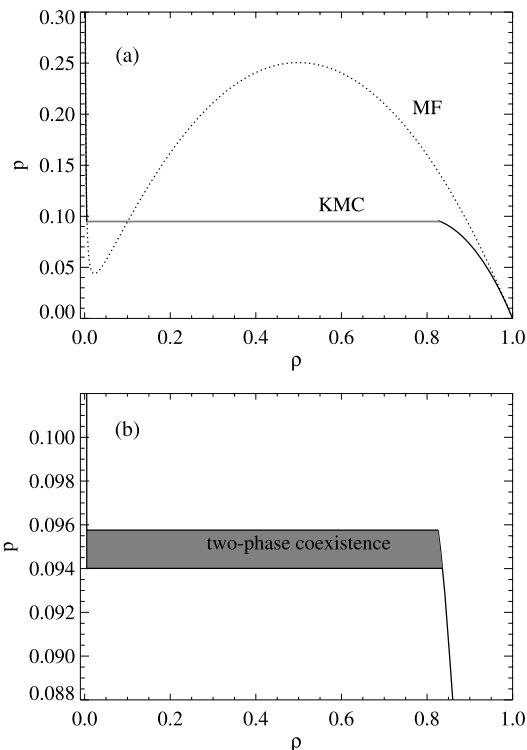
In Sect. 2, we presents results demonstrating generic two-phase coexistence in this model. In Sect. 3 we examine the criticality and related percolation issues. Concluding remarks are given in Sect. 4.

2 Generic Two-Phase Coexistence

To investigate the behavior of lattice-gas formulation of Schlögl second model, we perform kinetic Monte Carlo (KMC) simulations using two algorithms. The “normal” algorithm fixes all the physical rates (p , ε), then choose lattice site randomly and perform spontaneous annihilation/creation and autocatalytic creation processes according to their associated rates. However, for systems that exhibit first-order transitions, a constant-coverage algorithm [16] is proven to be more effective in determining key steady-state behavior. Here, we first introduce a target population density ρ^t . After randomly selecting a lattice-site, if the real density $\rho > \rho^t$, any particle on the lattice site is spontaneously annihilated; otherwise, if the site is vacant, either spontaneous or catalytic creation process is attempted, with rate ε and 1, respectively. The success rate of catalytic creation depends the number of occupied diagonal NN pairs. By keeping track of the total number of annihilation attempts $N_{\text{annihilation}}$ and creation attempts N_{creation} , the “effective” spontaneous annihilation rate can be obtained as $p_{\text{eff}} = N_{\text{annihilation}}/N_{\text{creation}}$. The “normal” and constant- ρ algorithm can be loosely associated with grand canonical and canonical ensemble of an equilibrium statistical system.

Figure 2 shows the KMC results using the constant- ρ algorithm of the model on a square lattice. Instead of a smooth cubic-like curve as in the MF solution, a horizontal tie-line connects the vacant and the reactive phases. Again, this is reminiscent of the Maxwell equal area construction of the van der Waals equation. If the population of the system lies between the steady-state coverage of the two phases ρ_{vacant} and ρ_{active} , the system will phase separate into domains of different phases. For the equilibrium liquid-vapor problem, the ordinate of

Fig. 2 (a) “Equation-of-state” of Schlögl’s second model for catalysis, with the spontaneous creation rate $\varepsilon = 0.0005$. The dotted line is the prediction of the MF theory, and the solid line is from KMC simulation using constant- ρ algorithm. (b) Blow up of the phase coexistence region. The shaded part is the generic two-phase coexistence region



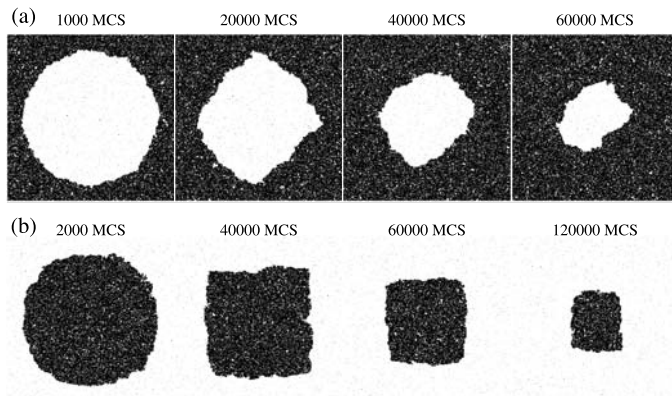


Fig. 3 Evolution of initially circular blobs inside a sea of the opposite phase, with the *same parameters* $\varepsilon = 0.0005$ and $p = 0.09488$. (a) A vacant blob; and (b) an active blob. A Monte Carlo sweep (MCS) corresponds to $1/(1 + p + \varepsilon)$ in “physical” time

the tie-line gives the equilibrium pressure of the liquid-vapor interface. At this pressure, both phases are equally stable, and a planar interface is stationary at the macroscopic level.

Surprisingly, closer inspections of the KMC results shows that equistable annihilation rate p_{eq} for a given ε is not a single value, but rather lies between a finite range of values (see Fig. 2b). The exact value of p_{eq} depends on the orientation of the interface between the vacant and the active phases. From constant coverage simulations of systems consisting of interfaces of different orientations, we find that for $\varepsilon = 0.0005$, p_{eq} ranges from $p_v = 0.09401$ for vertical or horizontal interfaces to $p_d = 0.09576$ for diagonal interfaces. For $p_v < p < p_d$, both the vacant and the active phases are genuinely stable rather than just metastable. In contrast, for equilibrium systems, it is generally expected that the first-order transition occurs only at a single point when the system is parameterized by a single variable. One can argue heuristically that if the free energy for the two phases has two different smooth forms, $F_1(\alpha)$ and $F_2(\alpha)$, that extend to metastable regime, then the phase coexistence occurs only at the intersection of the two curves. Existence of generic bistability or two-phase coexistence was first proved rigorously in a probabilistic cellular automata model by Toom [17, 18], and later found in other nonequilibrium models [19, 20]. Recently, the lattice-gas formulation of Schlögl’s second model for autocatalysis is also shown to exhibit generic phase coexistence [12], focusing on the case of $\varepsilon = 0$.

The case of $\varepsilon > 0$ provides a more general framework for studying nonequilibrium first-order transitions. Unlike the case with $\varepsilon = 0$, there is no absorbing phase with $\rho = 0$. The key feature of generic two-phase coexistence is in the dynamics of droplets embedded in a sea of the opposite phase. Genuine stability of the majority phase is ensured by the condition that droplets of the minority phase always shrink at the macroscopic level. This is true in our model for any $p_v < p < p_d$. Figure 3(a) shows snapshots of evolution of an initially circular blob of vacant phase with $\varepsilon = 0.0005$ and $p = 0.09488$ and Fig. 3(b) shows that of an active blob with the same parameters. With this value, for horizontal or vertical interfaces, the vacant phase is more stable, while for diagonal interfaces, the active phase is more stable. For a circular *vacant blob*, initially the horizontal or vertical parts of the blob grows while the diagonal part shrinks, thus the blob assumes a diamond shape. Subsequently it continues to shrink and disappear eventually. On the other hand, for a circular *active blob*, initially the diagonal part grows and the horizontal part shrinks, thus assuming a square shape. Then it continues to shrink and disappears eventually.

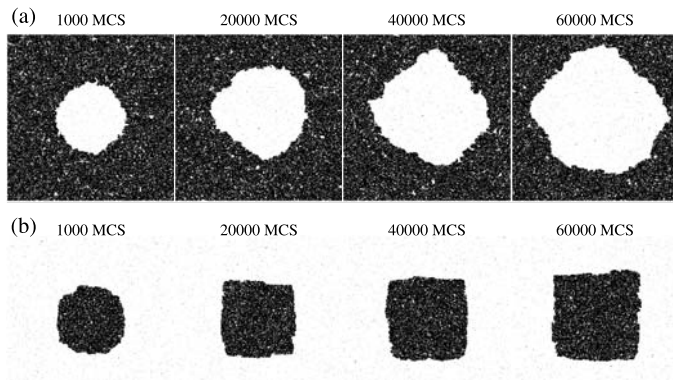


Fig. 4 Growth of initially circular blobs inside a sea of the opposite phase, with $\varepsilon = 0.0005$. **(a)** A vacant blob, with $p = 0.0966$; **(b)** an active blob, with $p = 0.0931$

For equilibrium systems, simultaneous shrinkage of a minority phases occurs only at the transition point. The driving force comes from interfacial tension coupled with curvature of the interface. In contrast, for the nonequilibrium model, simultaneous shrinkage of all minority phase occurs for a range of p values. Furthermore, after assuming their respective dynamical shapes (diamonds for vacant blobs, and squares for active blobs), the blobs shrink at a near constant rate in terms of their linear dimension, with the curvature effect of only secondary importance.

For p slightly outside the two-phase coexistence region, the system can be in a metastable state. As shown in Fig. 4, if $p > p_d$, a vacant blob will grow with a diamond shape, while if $p < p_v$, an active blob will grow with a square shape. As in the case of blob shrinkage, the shape of a growing blob is determined by the anisotropy in interface velocities through a “kinetic Wulff construction” as in the crystal growth problem. However, there is no equivalent equilibrium Wulff construction, as there does not exist a point where interfaces of all orientations are stationary.

Clearly, there is no symmetry between the two states (vacant and occupied) that a site can adopt in this model, which sets it apart from a class of irreversible models based on spin flip dynamics with “up-down” symmetry. For example, one can introduce a bias to the class of models in [21] in favor of one direction of spin versus the other. Due to the up-down symmetry of the spin dynamics, one expects phase coexistence only when the bias is zero. Therefore the lack of symmetry in Schlögl’s model for autocatalysis between vacant and occupied site is essential for generic two-phase coexistence. Incidentally, as mentioned in the introduction, a voter model based on Toom’s north-east-center majority rule [17, 18] does exhibit generic two-phase coexistence, however spatial symmetry is broken in this model.

It is tempting to suggest that Schlögl’s second model for autocatalysis provides the prototype for a class of nonequilibrium system with discontinuous phase transition without apparent symmetry between the two phases. It is therefore the nonequilibrium analog of the liquid-vapor phase transition. We conjecture that the Generic two-phase coexistence be a general feature for such systems. It should be interesting to investigate other models, e.g., the ZGB model for the $A + B_2$ surface reaction [22].

3 Nonequilibrium Criticality

As ε increases, the range of generic two-phase coexistence quickly decreases. Some preliminary results have been given in [12]. Here we provide more details. Figure 5 shows the range of equistable values of spontaneous annihilation rate for vertical interfaces p_v and diagonal interfaces p_d versus the spontaneous creation rate ε . The region between the two curves is the generic two-phase coexistence region. As shown in Fig. 5, this range decreases to zero rapidly as ε increases.

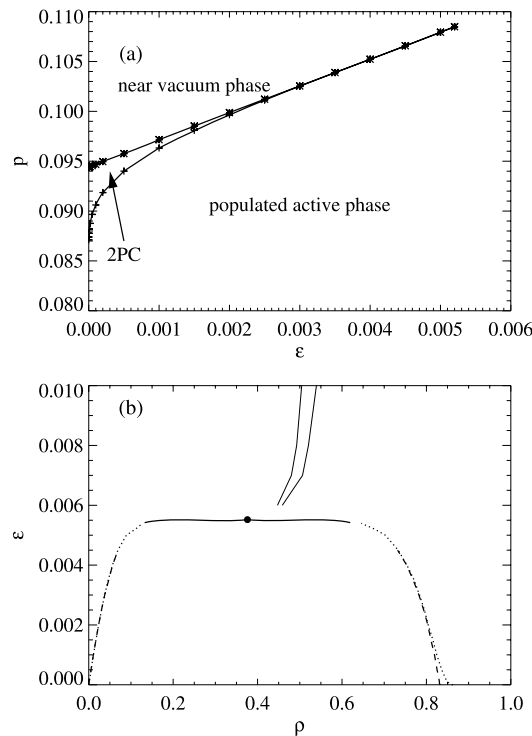
As mentioned above, from mean-field analysis, the spontaneous creation rate ε serves as a temperature-like variable. As ε increases to a critical value ε_c , the discontinuous transition becomes continuous with associated critical phenomena. It is widely expected that the criticality of a nonequilibrium continuous phase transition belongs to the universality class of the corresponding continuous equilibrium phase transition with the same symmetry and dimension. In this case, it is expected that near ε_c , the critical behavior will coincide with the two-dimensional Ising model.

This expectation is confirmed in our finite size scaling (FSS) analysis of fluctuations of the population, which based on the ansatz that near the critical point, a physical quantity such as fluctuations of a system with size $L \times L$ can be written as

$$\begin{aligned} \chi_L(t, h=0) &\equiv L^2(\langle \rho^2 \rangle - \langle \rho \rangle^2) \\ &\sim L^{\gamma/\nu} \tilde{\chi}[tL^{1/\nu}], \end{aligned} \quad (3)$$

where t and h are the temperature-like and external-field-like parameters. Due to lack of explicit symmetry of our model, they should be combinations of $\varepsilon - \varepsilon_c$ and $p - p_c$. An

Fig. 5 Phase diagram of the lattice-gas realization of the Schlögl's second model for autocatalysis on a square lattice. (a) In the (p, ε) plane. Results are from constant- ρ simulations using vertical interfaces (plotted with + signs) and using diagonal interfaces (* signs). (b) In the (ρ, ε) plane. There are two lines of phase coexistence curves, corresponding to the upper and lower transition lines in (a), drawn by a dashed line and a dotted line respectively. Results are from estimation of the density of different domains in constant- ρ simulations with vertical interfaces and diagonal interfaces. The solid line is a fit to the Ising curve $\rho_{\pm} = \rho_c + \Delta\rho(\varepsilon_c - \varepsilon)^{1/8}/2$. The solid circle denotes the critical point, estimated at $\rho_c = 0.375$ and $\varepsilon_c = 0.00552$. Also shown as two thinner lines are the percolation lines of clusters of vacant sites and occupied sites with NN connectivity. See text for details



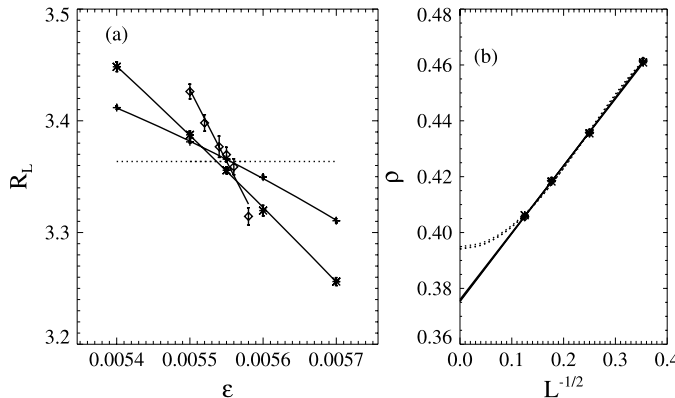


Fig. 6 (a) Finite-size scaling (FSS) analysis of fluctuations near criticality, plotting $R_L = \chi_{2L}/\chi_L$ along the maximal fluctuations loci versus ϵ , for $L = 8, 16$, and 32 . (b) Size scaling of the density at the maximal fluctuation loci for ϵ from 0.0054 to 0.0056 . The difference is indistinguishable on this scale. Extrapolation to $L \rightarrow \infty$ gives $\rho_c = 0.375(2)$. Also shown as dotted lines are fits to $1/L$ behavior

important step is to devise the so-called critical loci [23] in the (p, ϵ) plane that is the *asymptotic symmetry* line which is assumed to exist near the critical point. In this paper, for any given L , we use the p value that generates the largest χ , denoting it as p_L^* . Then we define

$$R_L(\epsilon) = \chi_{2L}(p_{2L}^*, \epsilon)/\chi_L(p_L^*, \epsilon). \quad (4)$$

By plotting R_L for different L 's, one can determine both ϵ_c and γ/ν from the crossing points of the curves. Using simulation data for $L = 8, 16$, and 32 , we obtain $\epsilon_c = 0.00552(3)$, $\gamma/\nu = 1.755(5)$, and $\nu = 0.96(5)$, in good agreement with the critical exponents of the two-dimensional Ising model with $\gamma = 7/4$ and $\nu = 1$. See Fig. 6(a). Simulation results with $L = 32$ and $L = 64$ suffer from significant uncertainties, mainly due to critical slowing-down of the dynamics. However, they are also consistent with the Ising exponents.

We can also extract the critical density ρ_c using the critical loci obtained above, translated into the (ρ, ϵ) plane and denoting the density where maximal fluctuations occurs as ρ_L^* for a given system size L . As shown in Fig. 6(b), significant finite-size effect exists and ρ_L^* seems to approach $\rho^*(L = \infty)$ as $L^{1/2}$. A linear fit to $L^{1/2}$ gives $\rho^*(L = \infty) = 0.376(1)$. However, this is somewhat different from the results for an three-dimensional equilibrium model for liquid-vapor transition [23] where there seems to be $(1/L)$ size corrections in ρ_L^* . Assuming $1/L$ corrections, the same data predicts $\rho^*(L = \infty) = 0.394$. At this stage, it is not clear to the author whether this unusual $L^{1/2}$ size correction is real, or just a crossover behavior. For comparison, the fit to $1/L$ is shown as a dotted line in Fig. 6(b). Figure 7 provides a snapshot of the system at the critical point.

It has been shown that for a variety of equilibrium systems that the continuous thermodynamic critical point coincides with the percolation transition (e.g., with T fixed at T_c) of suitably defined geometric clusters. The prime example is the Ising model where percolation of clusters of sites with the same spin and NN connectivity coincides with the Onsager critical point [24], and the critical exponents can be extracted from the tricritical $q = 1$ Potts model [25]. From Monte Carlo simulations, it seems that such a coincidence between percolation and order-disorder transitions is a more general phenomena [26–29]. One can ask a similar question for the nonequilibrium autocatalytic model, i.e., does the percolation

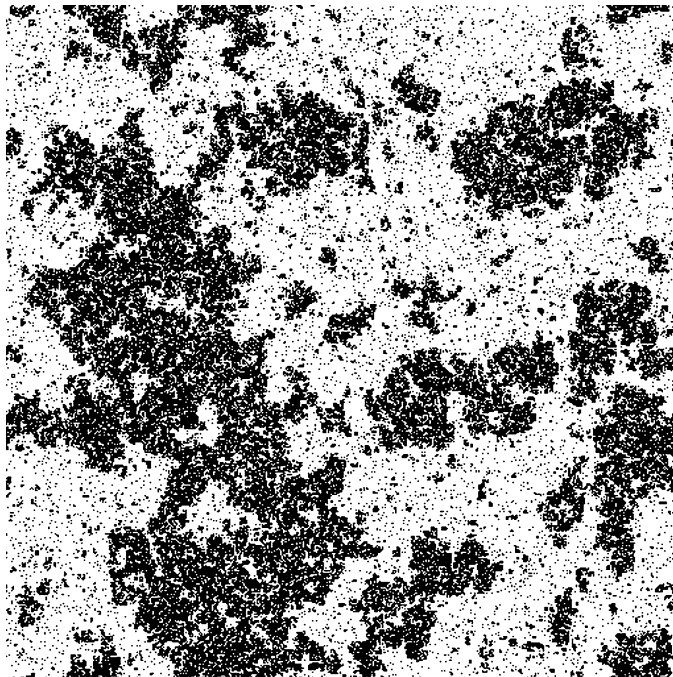


Fig. 7 Typical configuration near the critical point with $\varepsilon = 0.00552$ and $\rho = 0.376$. From constant- ρ simulations with $L = 512$

transition of clusters of either vacant or occupied sites with NN connectivity coincide with critical point (p_c, ε_c)? And if so, are the critical exponents the same as the Ising clusters? Figure 5(b) shows the percolation transition lines estimated using the spanning probability and constant- ρ simulations with $L = 256$ and $L = 512$. Starting at their random percolation threshold (0.407 and 0.593) for $\varepsilon = \infty$, the two transition lines come closer together as ε approach ε_c . However, accurate determination of percolation point suffers strongly from both larger correlation length and correlation time near the critical point. Finite-size scaling analysis of simulation data near the critical point with $\varepsilon = 0.00552$ and $L = 8$ to 64 suggests behavior closer to random percolation universality class, rather than exponents of an Ising cluster. It is possible that the two percolation lines does not completely close at the critical point. A more definitive answer will require a more accurate determination of the critical point and FSS analysis extending to larger system sizes.

4 Conclusions

We study the phase transitions in a simple two-dimensional lattice-gas model with non-equilibrium dynamics and show that the critical phenomena associated with the continuous transition belongs to the Ising universality class. However, due to the irreversible nature and the absence of any explicit “particle-hole” symmetry in the dynamic rule, instead of a single transition line, there is a finite region of the parameter space where phase coexistence occurs. It will be interesting to investigate other systems to see whether generic phase-coexistence is a general feature of nonequilibrium systems that exhibit phase separations and with no explicit symmetry between the phases.

Acknowledgements The author would like to thank J.W. Evans for extensive discussions and helps at every stage of this project. Work at the Ames Laboratory was supported by the Department of Energy, Basic Energy Sciences-Division of Chemical Sciences, under Contract No. DE-AC02-07CH11358.

References

1. Marro, J., Dickman, R.: *Nonequilibrium Phase Transitions in Lattice Models*. Cambridge University Press, Cambridge, (1999)
2. Hinrichsen, H.: *Adv. Phys.* **49**, 815 (2000)
3. Ódor, G.: *Rev. Mod. Phys.* **76**, 663 (2004)
4. Grinstein, G., Yayaprakash, C., He, Y.: *Phys. Rev. Lett.* **55**, 2527 (1985)
5. de Oliveira, M.J., Mendes, J.F.F., Santos, M.A.: *J. Phys. A* **26**, 2317 (1993)
6. Tomé, T., Dickman, R.: *Phys. Rev. E* **47**, 948 (1993)
7. Liu, D.J., Pavlenko, N., Evans, J.W.: *J. Stat. Phys.* **114**, 101 (2004)
8. Machado, E., Buendía, G.M., Rikvold, P.A., Ziff, R.M.: *Phys. Rev. E* **71**, 016120 (2005)
9. Liu, D.J., Evans, J.W.: *J. Chem. Phys.* **117**, 7319 (2002)
10. Machado, E., Buendía, G.M., Rikvold, P.A.: *Phys. Rev. E* **71**, 031603 (2005)
11. Durrett, R.: *SIAM Rev.* **41**, 677 (1999)
12. Liu, D.J., Guo, X., Evans, J.W.: *Phys. Rev. Lett.* **98**, 050601 (2007)
13. Guo, X., Liu, D.J., Evans, J.W.: *Phys. Rev. E* **75**, 061129 (2007)
14. Guo, X., Evans, J.W., Liu, D.J.: *Physica A* **387**, 177 (2008)
15. Schlögl, F.: *Z. Phys.* **253**, 147 (1972)
16. Brosilow, B.J., Ziff, R.M.: *Phys. Rev. A* **46**, 4534 (1992)
17. Toom, A.L.: In: Dobrushin, R.L., Sinai, Y.G. (eds.) *Multicomponent Random Systems. Advances in Probability and Related Topics*, vol. 6, pp. 549–575. Dekker, New York (1980), Chap. 18
18. Bennett, C.H., Grinstein, G.: *Phys. Rev. Lett.* **55**, 657 (1985)
19. Muñoz, M.A., de los Santos, F., da Gama, M.M.T.: *Eur. Phys. J. B* **43**, 73 (2005)
20. Hinrichsen, H., Livi, R., Mukamel, D., Politi, A.: *Phys. Rev. E* **61**, R1032 (2000)
21. Drouffe, J.M., Godréche, C.: *J. Phys. A* **32**, 249 (1999)
22. Ziff, R.M., Gulari, E., Barshad, Y.: *Phys. Rev. Lett.* **56**(24), 2553 (1986)
23. Orkoulas, G., Fisher, M.E., Panagiotopoulos, A.Z.: *Phys. Rev. E* **63**, 051507 (2001)
24. Coniglio, A., Klein, W.: *J. Phys. A* **13**, 2775 (1980)
25. Stella, A.L., Vandezande, C.: *Phys. Rev. Lett.* **62**, 1067 (1989)
26. Hu, C.K., Mak, K.S.: *Phys. Rev. B* **39**, 2948 (1989)
27. Liu, D.J., Evans, J.W.: *Phys. Rev. Lett.* **84**, 955 (2000)
28. Liu, D.J., Evans, J.W.: *Phys. Rev. B* **62**, 2134 (2000)
29. Fortunato, S.: *Phys. Rev. B* **67**, 014102 (2003)